Published by SET Publisher

Journal of Basic & Applied Sciences

ISSN (online): 1927-5129

Supporting Information

S1. METHODOLOGICAL APPROACH

1.1. Adiabatic Potential Energy Method

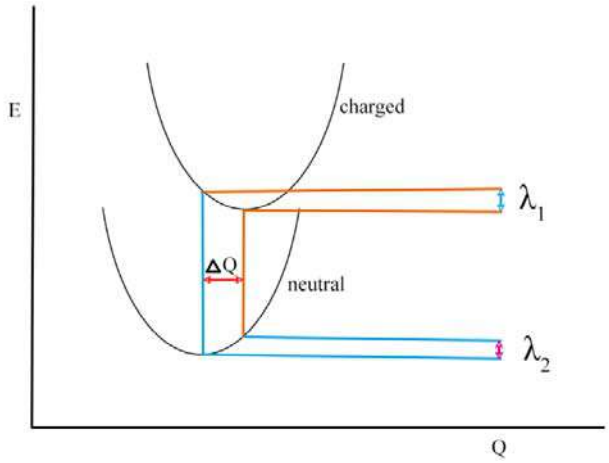

Figure S1: Schematic representation of the potential energy surfaces of the neutral and charged states with respect to the reaction coordinate.

Where the λ_1 is the difference between the charged state's minimum to the neutral state's potential energy and λ_2 is the difference between the neutral state's minimum to the charged sate's potential energy. We can know that λ_1 is not like λ_2 in figure 1. The normal model analyzes only the case of resonance. Here ΔQ is the normal mode displacement of the neutral state and charge state.

1.2. Super-Exchange Electronic Coupling

Our paper used the direct coupling method that minds we only consider donor HOMO (LUMO) orbital and accepter HOMO(LUMO) orbital. The other electronic coupling in D-A cocrystal has two computational methods. First one is energy splitting method [1]:

$$V_h^{eff} = (E_{HOMO}^{DAD} - E_{HOMO-1}^{DAD})/2 \ (1)$$

$$V_e^{eff} = (E_{LUMO+1}^{ADA} - E_{LUMO}^{ADA})/2 \ (2)$$

Where $E_{HOMO}^{DAD}(E_{LUMO}^{ADA})$ and $E_{HOMO-1}^{DAD}(E_{LUMO-1}^{ADA})$ is D-A-D(A-D-A) triad HOMO(LUMO+1) and HOMO-1(LUMO) energy. The energy splitting method has been widely used to evaluate two adjacent molecules [2] and in ambipolar D-A cocrystal also applies [3, 4]. Recently, many organic D-A cocrystals have shown good charge transport properties, which can be reasonably explained by super-exchange coupling from energy splitting calculations [3, 5-8]. The other one effective electronic coupling between adjacent D(A) is super-exchange can be written approximately as [9, 10]

$$t_h^{eff} = t_e^{eff} \approx \frac{t^2_{H_D-L_A}}{\Delta E} \quad (3)$$

In the above formula $t^2_{H_D-L_A}$ is the middle bridge molecule donor(acceptor) and adjacent two molecules acceptor(donor), therefore the molecular coupling is the same in a D-A-D tried. Here ΔE is charge transfer states energy, it represents the donor and acceptor the super-exchange interaction energy difference. We considered the molecule orbital coupling HOMO(LUMO) of the donor and acceptor molecule to study the charge transport properties.

S2. REORGANIZATION ENERGY

We calculate the DPTTA Duschinsky rotation matrix for the ground state and find that DPTTA is discrete in the 100 to 150 range. It minds normal mode analysis not suitable with DPTTA and we will know in normal model values and adiabatic potential energy methods values in table1. In table 1 we find that the adiabatic potential energy for DPTTA is 0.162 eV (λ_e) and 0.201 eV (λ_h) have large differences with normal model methods of 0.263 eV (λ_e) and 0.726 eV (λ_h). The results show our judgment is correct for DPTTA that DPTTA is not suitable with the normal model. But we did this job for normal model analysis in Figure 2 and give the Huang-Rhy factor in Figure 3.

Table 1: Reorganization energy (eV) calculate for hole and electron in adiabatic potential energy method and normal model

Compared	aP (λ_e)	aP (λ_h)	NM (λ_e)	NM (λ_h)
DPTTA	0.162	0.201	0.263	0.726
DPTTA in DPTTA-F_4TCNQ	0.162	0.201	0.261	0.715
F_4TCNQ in DPTTA-F_4TCNQ	0.256	0.157	0.257	0.157

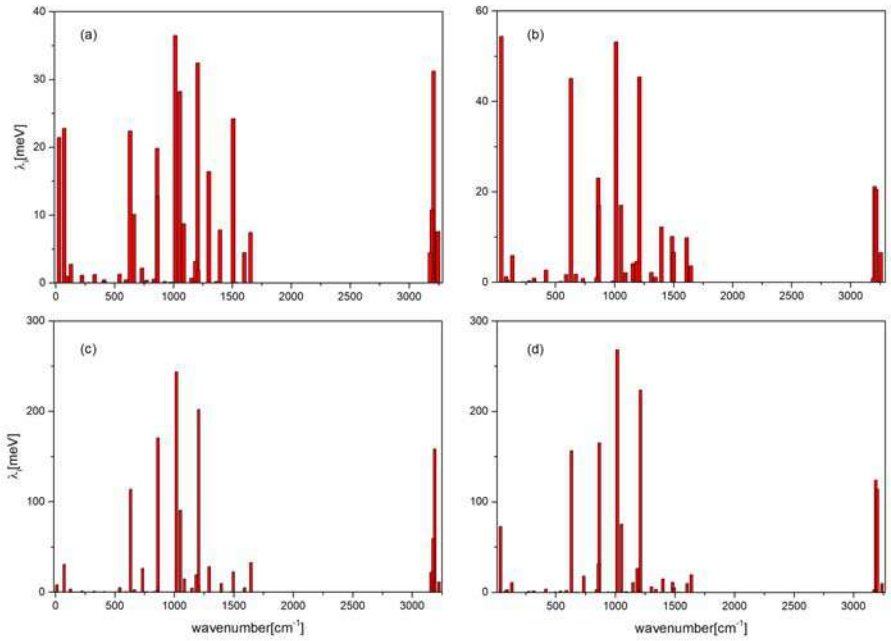

Figure 2: (a), (b). the reorganization energy contribution of DPTTA in the ground state and cation state in each vibrational mode. (c), (d) reorganization energy contribution of DPTTA molecule in the ground state and cation state in each vibrational mode of DPTTA-F_4TCNQ D-A complexes.

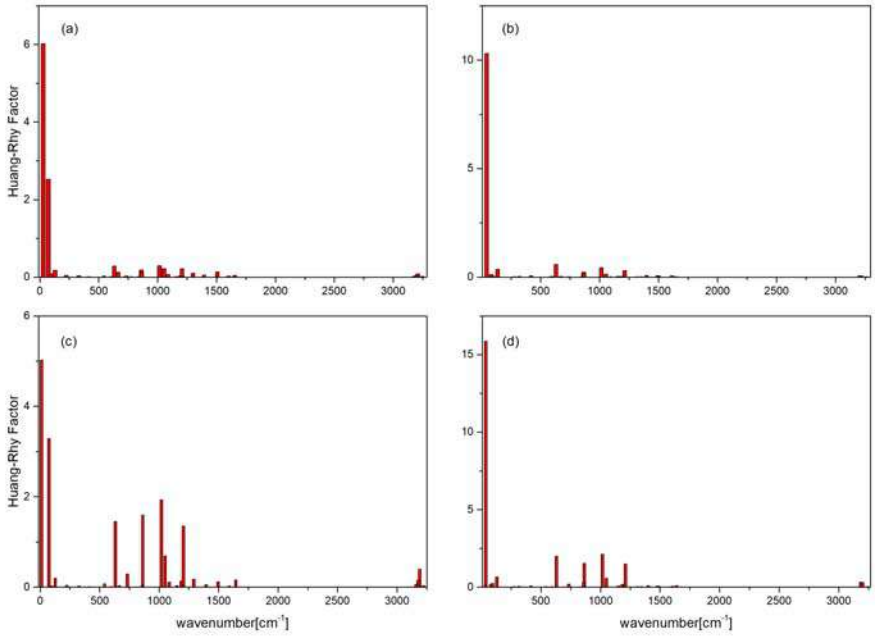

Figure 3: (a), (b). Huang-Rhys factors of DPTTA in each vibrational mode in ground state and cationic state. (c), (d) Huang-Rhys factor of DPTTA molecule in ground and cationic state of each vibrational mode in DPTTA-F_4TCNQ D-A complexes.

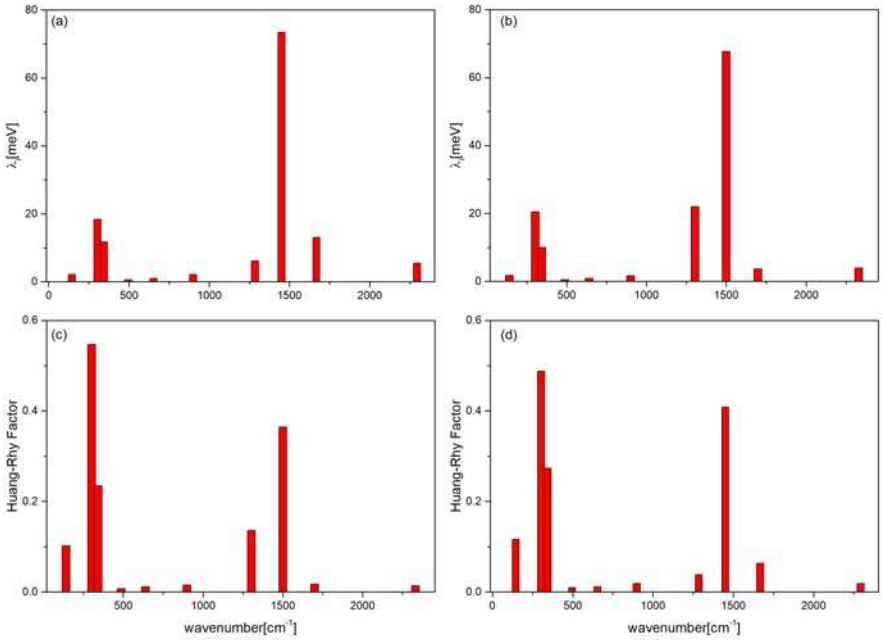

Figure 4: The molecular reorganization energy of F_4TCNQ in DPTTA-F_4TCNQ complexes is in (a) ground state (b) anion state and Huang-Rhys factor is in (c) ground state (d) anion state.

S3. CHARGE TRANSFER INTEGRALS

We calculate the transfer integrals of DPTTA single crystal and DPTTA-F_4TCNQ cocrystal, the detailed results we put in Table 2, Table 3, and Table 4. In articles, we plot the relationship between pathways and transfer integral. We can know that P11 and P12 are different from other integral values. For the appearance of the data in the table we can see Figure 5. The reason for P11 and P12 being larger than P15 and P16 are two conjugated skeletons relatively close together in Figure 5. In Figure 5 the P11 and P12 pathways can clearly view the dimer stack as parallel but the transfer integral in more lager. The molecular skeleton is close to each other although the molecular centers are getting farther apart. It's a reason why the molecular center distance increases but the transfer integral becomes larger. Another explanation is super-exchanger influences the transfer of integral values. In that direction the molecular stack is D-A-D conformity super-exchange occur situations.

Table 2: DPTTA calculated hole (V_h) and electron (V_e) transfer integral (meV) compared with literature and experiment in B3LYP/6-31G (d, p) level

Pathways	V_h	V_e	d
P1	-100.895	66.870	5.95
P2	-100.895	66.870	5.95
P3	4.269	-4.551	11.81
P4	4.269	-4.551	11.81
P5	4.269	-4.551	11.81
P6	4.269	-4.551	11.81
P7	-2.441	-0.786	12.85
P8	-2.441	-0.786	12.85
P9	-2.441	-0.786	12.85
P10	-2.441	-0.786	12.85
P11	0.019	-0.018	20.97
P12	0.019	-0.018	20.97

Table 3: DPTTA calculated hole (V_h) and electron (V_e) transfer integral (meV) in B3LYP/6-311G(d) level

Pathways	d	V_h	V_e
P1	3.973	-64.783	-37.119
P2	3.973	-64.783	-37.119
P3	10.099	49.083	-12.002
P4	10.099	49.083	-12.002
P5	10.365	-11.481	18.122
P6	10.365	-11.481	18.122
P7	11.251	6.741	-9.118
P8	11.251	6.741	-9.118
P9	12.019	2.716	6.043
P10	12.019	2.716	6.043
P11	12.499	-25.055	-18.478
P12	12.499	-25.055	-18.478
P13	14.874	-0.463	0.513
P14	14.874	-0.463	0.513

P15	15.509	-11.624	12.389
P16	15.509	-11.624	12.389
P17	17.071	-2.733	1.136
P18	17.071	-2.733	1.136

Table 4: F_4TCNQ calculated hole (V_h) and electron (V_e) transfer integral (meV) in B3LYP/6-311G(d) level.

Pathways	d	V_h	V_e
P1	3.973	-64.783	-37.119
P2	3.973	-64.783	-37.119
P3	10.365	-11.481	18.122
P4	10.365	-11.481	18.122
P5	12.499	-25.055	-18.478
P6	12.499	-25.055	-18.478
P7	15.509	-11.624	12.389
P8	15.509	-11.624	12.389

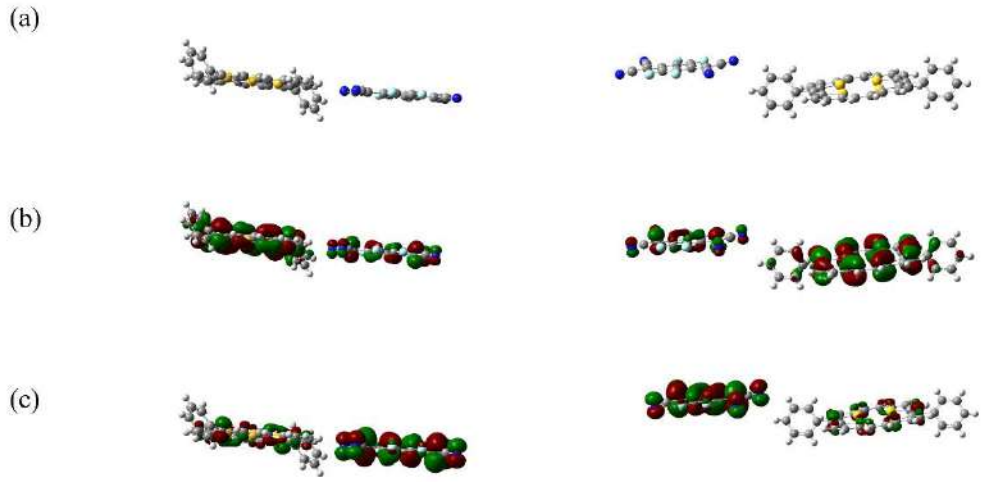

Figure 5: DPTTA and F_4TCNQ dimer P11, P12 pathways and P15, P16 pathways (a) molecular stack as well as they are HOMO orbital (b) and LUMO orbital (c).

REFERENCES

[1] J.-L. Brédas, J. P. Calbert, D. da Silva Filho, and J. Cornil, "Organic semiconductors: A theoretical characterization of the basic parameters governing charge transport," *Proceedings of the National Academy of Sciences,* vol. 99, no. 9, pp. 5804-5809, 2002.

[2] V. Coropceanu, J. Cornil, D. A. Da Silva Filho, Y. Olivier, R. Silbey, and J. L. Brédas, "Erratum: Charge transport in organic semiconductors (Chemical Reviews (2007) vol. 107 (926-952))," *Chemical Reviews,* vol. 107, no. 5, p. 2165, 2007.

[3] J. Zhang *et al.*, "Sulfur-Bridged Annulene-TCNQ Co-Crystal: A Self-Assembled ‘‘Molecular Level Heterojunction’’with Air Stable Ambipolar Charge Transport Behavior," *Advanced Materials,* vol. 24, no. 19, pp. 2603-2607, 2012.

[4] H. Zhu, E. S. Shin, A. Liu, D. Ji, Y. Xu, and Y. Y. Noh, "Printable semiconductors for backplane TFTs of flexible OLED displays," *Advanced Functional Materials,* vol. 30, no. 20, p. 1904588, 2020.

[5] S. K. Park *et al.*, "Tailor-made highly luminescent and ambipolar transporting organic mixed stacked charge-transfer crystals: an isometric donor–acceptor approach," *Journal of the American Chemical Society,* vol. 135, no. 12, pp. 4757-4764, 2013.

[6] K. Iijima, R. Sanada, D. Yoo, R. Sato, T. Kawamoto, and T. Mori, "Carrier Charge Polarity in Mixed-Stack Charge-Transfer Crystals Containing Dithienobenzodithiophene," *ACS applied materials & interfaces,* vol. 10, no. 12, pp. 10262-10269, 2018.

[7] Y. Qin *et al.*, "Efficient ambipolar transport properties in alternate stacking donor–acceptor complexes: from experiment to theory," *Physical Chemistry Chemical Physics,* vol. 18, no. 20, pp. 14094-14103, 2016.

[8] Y. Qin *et al.*, "Charge-transfer complex crystal based on extended-π-conjugated acceptor and sulfur-bridged annulene: charge-transfer interaction and remarkable high ambipolar transport characteristics," *Advanced Materials,* vol. 26, no. 24, pp. 4093-4099, 2014.

[9] X. Chen, H. Wang, B. Wang, Y. Wang, X. Jin, and F.-Q. Bai, "Charge transport properties in organic DA mixed-stack complexes based on corannulene and sumanene derivatives-a theoretical study," *Organic Electronics,* vol. 68, pp. 35-44, 2019.

[10] L. Zhu, Y. Yi, A. Fonari, N. S. Corbin, V. Coropceanu, and J.-L. Brédas, "Electronic properties of mixed-stack organic charge-transfer crystals," *The Journal of Physical Chemistry C,* vol. 118, no. 26, pp. 14150-14156, 2014.